

ANALYSIS & PDE

Volume 10 No. 2 2017

DIEGO CORDOBA, JAVIER GÓMEZ-SERRANO AND ANDREJ ZLATOŠ

**A NOTE ON STABILITY SHIFTING FOR THE MUSKAT PROBLEM,
II:
FROM STABLE TO UNSTABLE AND BACK TO STABLE**

A NOTE ON STABILITY SHIFTING FOR THE MUSKAT PROBLEM, II: FROM STABLE TO UNSTABLE AND BACK TO STABLE

DIEGO CÓRDOBA, JAVIER GÓMEZ-SERRANO AND ANDREJ ZLATOŠ

In this note, we show that there exist solutions of the Muskat problem which shift stability regimes in the following sense: they start stable, then become unstable, and finally return back to the stable regime. This proves the existence of double stability shifting in the direction opposite to (as well as more difficult and more surprising than) the one shown by Cordoba et al. (*Philos. Trans. Roy. Soc. A* **373**:2050 (2015), art. id. 20140278).

1. Introduction

In this paper, we study two incompressible fluids with the same viscosity but different densities, ρ^+ and ρ^- , evolving in a two-dimensional porous medium with constant permeability κ . The velocity v is determined by Darcy's law

$$\mu \frac{v}{\kappa} = -\nabla p - g \begin{pmatrix} 0 \\ \rho \end{pmatrix}, \quad (1-1)$$

where p is the pressure, $\mu > 0$ viscosity, and $g > 0$ gravitational acceleration. In addition, v is incompressible:

$$\nabla \cdot v = 0. \quad (1-2)$$

By rescaling properly, we can assume $\kappa = \mu = g = 1$. The fluids also satisfy the conservation of mass equation

$$\partial_t \rho + v \cdot \nabla \rho = 0. \quad (1-3)$$

This is known as the Muskat problem [1937]. We denote by Ω^+ the region occupied by the fluid with density ρ^+ and by Ω^- the region occupied by the fluid with density $\rho^- \neq \rho^+$. The point $(0, \infty)$ belongs to Ω^+ , whereas the point $(0, -\infty)$ belongs to Ω^- . All quantities with superindex \pm will refer to Ω^\pm respectively. The interface between both fluids at any time t is a planar curve $z(\cdot, t)$. We will work in the setting of horizontally periodic interfaces, although our results can be extended to the flat-at-infinity case.

A quantity that will play a major role in this paper is the Rayleigh–Taylor condition, which is defined as

$$\text{RT}(x, t) = -[\nabla p^-(z(x, t)) - \nabla p^+(z(x, t))] \cdot \partial_x^\perp z(x, t),$$

where we use the convention $(u, v)^\perp = (-v, u)$. If $\text{RT}(x, t) > 0$ for all $x \in \mathbb{R}$, then we say that the curve is in the Rayleigh–Taylor stable regime at time t , and if $\text{RT}(x, t) \leq 0$ for some $x \in \mathbb{R}$, then we say that the curve is in the Rayleigh–Taylor unstable regime.

MSC2010: primary 35Q35; secondary 35R35, 65G30, 76B03.

Keywords: Muskat problem, interface, incompressible fluid, porous media, Rayleigh–Taylor, computer-assisted.

One can rewrite the system (1-1)–(1-3) in terms of the curve $z = (z^1, z^2)$, obtaining

$$\partial_t z(x, t) = \frac{\rho^- - \rho^+}{2\pi} \text{P.V.} \int_{\mathbb{R}} \frac{z^1(x, t) - z^1(y, t)}{|z(x, t) - z(y, t)|^2} (\partial_x z(x, t) - \partial_y z(y, t)) dy. \quad (1-4)$$

In the horizontally periodic case with $z(x + 2\pi, t) = z(x, t) + (2\pi, 0)$, the formula

$$\frac{1}{2} \cot \frac{y}{2} = \frac{1}{y} + \sum_{n=1}^{\infty} \frac{2y}{y^2 - (2\pi n)^2}$$

can be used to show [Castro et al. 2012] that the velocity satisfies

$$\partial_t z(x, t) = \frac{\rho^- - \rho^+}{4\pi} \int_{\mathbb{T}} \frac{\sin(z^1(x, t) - z^1(y, t)) (\partial_x z(x, t) - \partial_y z(y, t))}{\cosh(z^2(x, t) - z^2(y, t)) - \cos(z^1(x, t) - z^1(y, t))} dy. \quad (1-5)$$

A simple calculation of the Rayleigh–Taylor condition in terms of z yields

$$\text{RT}(x, t) = (\rho^- - \rho^+) \partial_x z^1(x, t).$$

When the interface is a graph, parametrized as $z(x, t) = (x, f(x, t))$, equation (1-4) becomes

$$\partial_t f(x, t) = \frac{\rho^- - \rho^+}{4\pi} \int_{\mathbb{T}} \frac{\sin(x - y) (\partial_x f(x, t) - \partial_y f(y, t))}{\cosh(f(x, t) - f(y, t)) - \cos(x - y)} dy \quad (1-6)$$

and the Rayleigh–Taylor condition simplifies to

$$\text{RT}(x, t) = \rho^- - \rho^+.$$

The curve is now in the RT stable regime whenever $\rho^+ < \rho^-$; that is, the denser fluid is at the bottom. From now on, we assume that $\rho^- - \rho^+ = 4\pi$, which can be done after an appropriate scaling in time.

The Muskat problem has been studied in many works. A proof of local existence of classical solutions in the Rayleigh–Taylor stable regime in H^3 and ill-posedness in the unstable regime appears in [Córdoba and Gancedo 2007]. See also [Constantin et al. 2016b] for an improvement on the regularity (to $W^{2,p}$ spaces). In the one-phase case (i.e., when one of the densities and permeabilities is zero) local existence in H^2 was proved in [Cheng et al. 2016].

A maximum principle for $\|\partial_x f(\cdot, t)\|_{L^\infty}$ can be found in [Córdoba and Gancedo 2009]. Moreover, the authors showed in [Córdoba and Gancedo 2009] that if $\|\partial_x f_0\|_{L^\infty} < 1$, then $\|\partial_x f(\cdot, t)\|_{L^\infty} \leq \|\partial_x f_0\|_{L^\infty}$ for all $t > 0$. Further work has shown existence of finite-time turning [Castro et al. 2012] (i.e., the curve ceases to be a graph in finite time and the Rayleigh–Taylor condition changes sign to negative somewhere along the curve). The gap between these two results (i.e., the question whether the constant 1 is sharp or not for guaranteeing global existence) is still an open question, and there is numerical evidence of data with $\|\partial_x f_0\|_{L^\infty} = 50$ which turns over [Córdoba et al. 2015].

As was demonstrated in [Castro et al. 2013], the curve may lose regularity after shifting from the stable regime to the unstable regime. However, the possibility of it recoiling and returning to the stable regime has not been excluded. The occurrence of this phenomenon is the main result of this note, Theorem 2.1. (In Theorem 2.3 we also extend this to a proof of existence of the quadruple stability shift scenario unstable \rightarrow stable \rightarrow unstable \rightarrow stable \rightarrow unstable.) In [Córdoba et al. 2015] we showed that there

exist curves which undergo the unstable \rightarrow stable \rightarrow unstable transition, so this settles the question about existence of double stability shift scenarios in both directions. We stress that existence of the stable \rightarrow unstable \rightarrow stable scenario is in fact by no means expected, as well as considerably more challenging to establish than the unstable \rightarrow stable \rightarrow unstable one.

More general models, which take into account finite depth or nonconstant permeability, and which also exhibit (single) turning were studied in [Berselli et al. 2014; Gómez-Serrano and Granero-Belinchón 2014]. The estimates in [Gómez-Serrano and Granero-Belinchón 2014] were carried out by rigorous computer-assisted methods, as opposed to the traditional pencil and paper ones in [Berselli et al. 2014].

Concerning global existence, the first proof for small initial data was carried out in [Siegel et al. 2004] in the case where the fluids have different viscosities and the same densities (see also [Córdoba and Gancedo 2007] for the setting of the present paper — different densities and the same viscosities — and also [Cheng et al. 2016] for the general case). Global existence for medium-sized initial data was established in [Constantin et al. 2013; 2016a]. In the case where surface tension is taken into account, global existence was shown in [Escher and Matioc 2011; Friedman and Tao 2003]. Global existence for the confined case was treated in [Granero-Belinchón 2014]. A blow-up criterion was found in [Constantin et al. 2016b].

Recent advances in computing power have made possible rigorous computer-assisted proofs. Of course, floating-point operations can result in numerical errors, and we will employ interval arithmetics to deal with this issue. Instead of working with arbitrary real numbers, we perform computations over intervals which have representable numbers as endpoints. On these objects, an arithmetic is defined in such a way that we are guaranteed that for every $x \in X, y \in Y$,

$$x \star y \in X \star Y$$

for any operation \star . For example,

$$\begin{aligned} [\underline{x}, \bar{x}] + [\underline{y}, \bar{y}] &= [\underline{x} + \underline{y}, \bar{x} + \bar{y}], \\ [\underline{x}, \bar{x}] \times [\underline{y}, \bar{y}] &= [\min\{\underline{x}\underline{y}, \underline{x}\bar{y}, \bar{x}\underline{y}, \bar{x}\bar{y}\}, \max\{\underline{x}\underline{y}, \underline{x}\bar{y}, \bar{x}\underline{y}, \bar{x}\bar{y}\}]. \end{aligned}$$

We can also define the interval version of a function $f(X)$ as an interval I that satisfies that for every $x \in X$, we have $f(x) \in I$. Rigorous computation of integrals has been theoretically developed since the seminal works of Moore and many others (see [Berz and Makino 1999; Krämer and Wedner 1996; Lang 2001; Moore 1979; Tucker 2011] for just a small sample). For readability purposes, instead of writing the intervals as, for instance, $[123456, 123789]$, we will sometimes instead refer to them as 123_{789}^{456} .

This note is organized as follows. In Section 2 we prove Theorems 2.1 and 2.3, and in Section 3 we provide technical details regarding the performance and implementation of the computations. The appendix, found in an online supplement, contains a detailed derivation and enumeration of all the necessary integrals which have to be rigorously computed, their enclosures, and the performance of the computations.

2. The main result

The following theorem is the main result of this paper (see also Theorem 2.3 below).

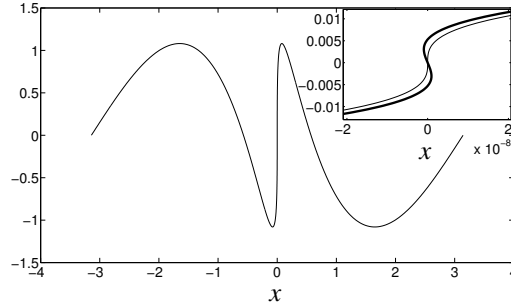


Figure 1. The curve $z_\varepsilon(x, 0)$ from Lemma 2.2 with $A(\varepsilon) = 1.08050$. Inset: closeup around $x = 0$. Thick curve: $\varepsilon = 10^{-6}$, thin curve: $\varepsilon = 0$. We remark that both curves are indistinguishable at the larger scale.

Theorem 2.1. *There exist $T > \gamma > 0$ and a spatially analytic solution z to (1-5) on the time interval $[-T, T]$ such that $z(\cdot, t)$ is a graph of a smooth function of x when $|t| \in [T - \gamma, T]$ (i.e., z is in the stable regime near $t = \pm T$) but $z(\cdot, t)$ is not a graph of a function of x when $|t| \leq \gamma$ (i.e., z is in the unstable regime near $t = 0$).*

The intuition behind this result comes from the numerical experiments which were started in [Córdoba et al. 2015]. These suggested existence of curves which are (barely) in the unstable regime, and such that the evolution both forward and backwards in time transports them into the stable regime. (We note that neither the velocity nor any other quantity was observed to become degenerate in these experiments). We remark that this behavior is purely nonlinear and thus nonlinear effects may dominate the linear ones under certain conditions. The following lemma constructs a family of such curves (see Figure 1).

Lemma 2.2. *Let $\varepsilon \geq 0$ and consider the initial curve $z_\varepsilon(x, 0) = (z_\varepsilon^1(x, 0), z_\varepsilon^2(x, 0))$, with*

$$z_\varepsilon^1(x, 0) = x - \sin(x) - \varepsilon \sin(x) \quad \text{and} \quad z_\varepsilon^2(x, 0) = A(\varepsilon) \sin(2x).$$

(1) *For any $\varepsilon \in [0, 10^{-6}]$, there exists $A(\varepsilon) \in (1.08050, 1.08055)$ such that if z_ε solves (1-5) with initial data $z_\varepsilon(x, 0)$, then*

$$\partial_t \partial_x z_\varepsilon^1(0, 0) = 0.$$

(2) *There are $T > 0$ and $C \geq 1$, independent of ε , such that for any $\varepsilon \in [0, 10^{-6}]$ and $A(\varepsilon)$ from (1), there is a unique analytic solution z_ε of (1-5) on the time interval $(-T, T)$ with initial data $z_\varepsilon(x, 0)$, and it satisfies*

$$\partial_{tt} \partial_x z_\varepsilon^1(0, 0) \geq 30, \tag{2-1}$$

as well as

$$|\partial_t \partial_x z_\varepsilon^1(x, t)| + |\partial_t \partial_x^3 z_\varepsilon^1(x, t)| + |\partial_t^2 \partial_x^2 z_\varepsilon^1(x, t)| + |\partial_t^3 \partial_x z_\varepsilon^1(x, t)| \leq C \tag{2-2}$$

for each $(x, t) \in \mathbb{T} \times (-T, T)$.

Proof. The proofs of (1) and (2-1) are computer-assisted, and the codes can be found in the online supplement.

Let us start with (1). Since $\partial_t \partial_x z_\varepsilon^1(0, 0)$ (i.e., the spatial derivative of the first coordinate of the right-hand side of (1-5) at $(x, t) = (0, 0)$) is a continuous function of $A(\varepsilon)$, it suffices to show that the signs of $\partial_t \partial_x z_\varepsilon^1(0, 0)$ for $A(\varepsilon) = 1.08050$ and for $A(\varepsilon) = 1.08055$ are different for each $\varepsilon \in [0, 10^{-6}]$. This holds because for each such ε we obtain the bounds

$$\begin{aligned} \partial_t \partial_x z_\varepsilon^1(0, 0) &\in 0.000_{27}^{01} \quad \text{for } A(\varepsilon) = 1.08050, \\ \partial_t \partial_x z_\varepsilon^1(0, 0) &\in -0.000_{02}^{28} \quad \text{for } A(\varepsilon) = 1.08055. \end{aligned} \tag{2-3}$$

Existence and uniqueness of the solution z_ε in (2) follows directly from the proof of Theorem 5.1 in [Castro et al. 2012], which proves local well-posedness for (1-5) in the class of analytic functions of x . The time $T > 0$ is then uniform in all small ε (and $\sup_{|t| < T} \|\partial_x^k z_\varepsilon(\cdot, t)\|_{L^\infty}$ is also uniformly bounded for each k) because the same is true for all the estimates in that proof.

Then (2-1) follows by taking $A(\varepsilon) = [1.08050, 1.08055]$ (the full interval, since we do not know $A(\varepsilon)$ explicitly) and propagating this interval in the relevant computations. Specifically, we obtain

$$\partial_{tt} \partial_x z_\varepsilon^1(0, 0) \in [38.706, 48.787].$$

The proof of Theorem 5.1 in [Castro et al. 2012] shows that the chord-arc constant

$$\sup_{x, y \in \mathbb{T}, y \neq 0} \frac{|y|}{|z_\varepsilon(x, t) - z_\varepsilon(x - y, t)|}$$

(where $\mathbb{T} = [-\pi, \pi]$ with $\pm\pi$ identified) is bounded uniformly in all ε, t under consideration (provided $T > 0$ is small enough). Thus there is $D < \infty$ such that

$$\left| \frac{1}{\cosh(z_\varepsilon^2(x, t) - z_\varepsilon^2(x - y, t)) - \cos(z_\varepsilon^1(x, t) - z_\varepsilon^1(x - y, t))} \right| \leq \frac{D}{y^2}$$

for all these ε, t and all $x, y \in \mathbb{T}$. This allows us to obtain (2-2) by brute force, differentiating and estimating all the resulting terms separately. The most singular term in $\partial_t \partial_x^j z_\varepsilon^1(x, t)$ ($j = 1, 3$) is

$$\int_{\mathbb{T}} \frac{\sin(z_\varepsilon^1(x, t) - z_\varepsilon^1(x - y, t))(\partial_x^{j+1} z_\varepsilon^1(x, t) - \partial_x^{j+1} z_\varepsilon^1(x - y, t))}{\cosh(z_\varepsilon^2(x, t) - z_\varepsilon^2(x - y, t)) - \cos(z_\varepsilon^1(x, t) - z_\varepsilon^1(x - y, t))} dy \leq 2\pi D \|\partial_x^{j+2} z_\varepsilon^1(\cdot, t)\|_{L^\infty} \leq C$$

for some C which is uniform in ε due to the above-mentioned uniform bounds on $\|\partial_x^k z_\varepsilon(\cdot, t)\|_{L^\infty}$. Analogously, the most singular term in $\partial_t^2 \partial_x^2 z_\varepsilon^1(x, t)$ is given by

$$\int_{\mathbb{T}} \frac{\sin(z_\varepsilon^1(x, t) - z_\varepsilon^1(x - y, 0))(\partial_t \partial_x^3 z_\varepsilon^1(x, t) - \partial_t \partial_x^3 z_\varepsilon^1(x - y, t))}{\cosh(z_\varepsilon^2(x, t) - z_\varepsilon^2(x - y, t)) - \cos(z_\varepsilon^1(x, t) - z_\varepsilon^1(x - y, t))} dy \leq 2\pi D \|\partial_t \partial_x^4 z_\varepsilon^1(\cdot, t)\|_{L^\infty},$$

and the last term can be bounded by a uniform C in the same way as $\partial_t \partial_x^3 z_\varepsilon^1(x, t)$. Finally, the most singular term in $\partial_t^3 \partial_x z_\varepsilon^1(x, t)$ is

$$\int_{\mathbb{T}} \frac{\sin(z_\varepsilon^1(x, t) - z_\varepsilon^1(x - y, t))(\partial_t^2 \partial_x^2 z_\varepsilon^1(x, t) - \partial_t^2 \partial_x^2 z_\varepsilon^1(x - y, t))}{\cosh(z_\varepsilon^2(x, t) - z_\varepsilon^2(x - y, t)) - \cos(z_\varepsilon^1(x, t) - z_\varepsilon^1(x - y, t))} dy \leq 2\pi D \|\partial_t^2 \partial_x^3 z_\varepsilon^1(\cdot, t)\|_{L^\infty},$$

which is bounded by a uniform C in the same way as $\partial_t^2 \partial_x^2 z_\varepsilon^1(x, t)$ (with the bound this time involving the uniformly bounded quantity $\|\partial_x^7 z_\varepsilon^1(\cdot, t)\|_{L^\infty}$). □

Proof of Theorem 2.1. Let T, C be from Lemma 2.2. Then (2-2) shows that for any small enough $\varepsilon > 0$ and any $|t| \leq \sqrt{\varepsilon}$ and $|x| \in [2C^{1/2}\varepsilon^{1/4}, \pi]$ we have $\partial_x z_\varepsilon^1(x, t) > 0$. Indeed, this is because

$$1 - (1 + \varepsilon) \cos(2C^{1/2}\varepsilon^{1/4}) - C\sqrt{\varepsilon} > 0$$

when $\varepsilon > 0$ is small (since C is fixed).

Next let $|t| \leq \sqrt{\varepsilon}$ and $|x| \leq 2C^{1/2}\varepsilon^{1/4}$. Then there are $|x^\sharp|, |x^{\sharp\sharp}| \leq |x|$ and $|t^\sharp| \leq \sqrt{\varepsilon}$ such that

$$\begin{aligned} \partial_x z_\varepsilon^1(x, t) &= \partial_x z_\varepsilon^1(x, 0) + t\partial_t \partial_x z_\varepsilon^1(x, 0) + \frac{1}{2}t^2 \partial_t^2 \partial_x z_\varepsilon^1(x, 0) + \frac{1}{6}t^3 \partial_t^3 \partial_x z_\varepsilon^1(x, t^\sharp) \\ &= -\varepsilon \cos(x) + [1 - \cos(x)] + t[\partial_t \partial_x z_\varepsilon^1(0, 0) + x\partial_t \partial_x^2 z_\varepsilon^1(0, 0) + \frac{1}{2}x^2 \partial_t \partial_x^3 z_\varepsilon^1(x^\sharp, 0)] \\ &\quad + \frac{1}{2}t^2 [\partial_t^2 \partial_x z_\varepsilon^1(0, 0) + x\partial_t^2 \partial_x^2 z_\varepsilon^1(x^{\sharp\sharp}, 0)] + \frac{1}{6}t^3 \partial_t^3 \partial_x z_\varepsilon^1(x, t^\sharp) \\ &\geq -\varepsilon + x^2(\frac{1}{4} - \frac{1}{2}C|t|) + t^2(15 - \frac{1}{2}C|x| - \frac{1}{6}C|t|), \end{aligned}$$

where we used the estimates from Lemma 2.2 and also that $\partial_t \partial_x^2 z_\varepsilon^1(0, 0) = 0$ by oddness of z_ε . Since $|t| \leq \sqrt{\varepsilon}$ and $|x| \leq 2C^{1/2}\varepsilon^{1/4}$, taking small enough $\varepsilon > 0$ now yields $\partial_x z_\varepsilon^1(x, t) \geq 14t^2 - \varepsilon > 0$ for all $|t| \in [\frac{1}{2}\sqrt{\varepsilon}, \sqrt{\varepsilon}]$ and $|x| \leq 2C^{1/2}\varepsilon^{1/4}$. The theorem then follows with $z = z_\varepsilon$, $T = \sqrt{\varepsilon}$, and $\gamma = \varepsilon/(2C)$ for such ε (here we also used (2-2) and $\partial_x z_\varepsilon^1(0, 0) = -\varepsilon$). \square

We next show that our approach allows for the proof of existence of solutions which exhibit even more complicated stability shifting. We will construct a solution with an unstable \rightarrow stable \rightarrow unstable \rightarrow stable \rightarrow unstable stability regime profile.

We start by noticing that it suffices to consider solutions to (1-4) with periodicity of the form

$$z(x + 8N\pi, t) = z(x, t) + (8N\pi, 0)$$

for some integer $N \geq 1$, because then $\tilde{z}(x, t) = 1/(4N)z(4Nx, 4Nt)$ also solves (1-4) and $\tilde{z}(x + 2\pi, t) = \tilde{z}(x, t) + (2\pi, 0)$. Our initial data will be a perturbation of the $8N\pi$ -periodic extension of the odd function

$$z(x, 0) = \bar{z}_{A(0)}(x)\chi_{[0, N\pi]}(|x|) + \bar{z}_{1.08055}(x)\chi_{(N\pi, 3N\pi]}(|x|) + \bar{z}_{1.08050}(x)\chi_{(3N\pi, 4N\pi]}(|x|), \tag{2-4}$$

with $\bar{z}_B(x) = (x - \sin x, B \sin(2x))$ and $A(0) \in (1.08050, 1.08055)$ from Lemma 2.2. If N is large, the estimates from the lemma and its proof show that at time $t = 0$, the corresponding solution wants to make the shifts stable \rightarrow unstable \rightarrow stable at $x = 0$, stable \rightarrow unstable at $|x| = 2N\pi$, and unstable \rightarrow stable at $|x| = 4N\pi$. An appropriate perturbation of this initial data, which makes the unstable phase of the first shift last a positive length of time, delays the second shift, and brings the third shift forward in time, would then achieve our goal.

We will also need this perturbation to resolve some other issues. Specifically, the initial condition must be analytic so that we can solve the PDE both forward and backward in time, and the solution must remain stable near $x = 2n\pi$ for any integer n with $|n| \in (0, 2N) \setminus \{N\}$ (note that the tangent to $z(\cdot, 0)$ is vertical at these points). For any large N we therefore let

$$B_{N,A}(x)$$

$$= [A + (1.08055 - A)\phi(|x| - N\pi)]\chi_{[0, 3N\pi]}(|x|) + [1.08050 + 0.00005\phi(3N\pi + 1 - |x|)]\chi_{(3N\pi, 4N\pi]}(|x|),$$

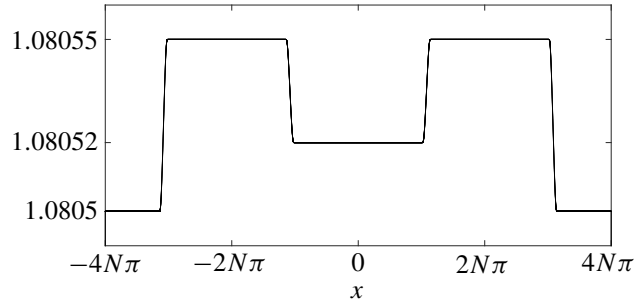


Figure 2. $B_{N,A}(x)$ for $A = 1.08052$.

with $A \in [1.08050, 1.08055]$ and $0 \leq \phi \leq 1$ smooth such that $\phi(y) = 0$ for $y \leq 0$ and $\phi(y) = 1$ for $y \geq 1$, and we extend $B_{N,A}$ to \mathbb{R} periodically (with period $8N$). See Figure 2 for a depiction of $B_{N,A}(x)$. Next we let δ_y be the delta function at $y \in \mathbb{R}$, and define the $8N\pi$ -periodic odd functions

$$\bar{z}_{N,A}(x) = (x - \sin x, B_{N,A}(x) \sin(2x))$$

and

$$z_{N,A,r,a,c}(\cdot, 0) = P_r * \bar{z}_{N,A} + P_1 * (a\beta_{N,0} + c\beta_{N,2N\pi} + c\beta_{N,-2N\pi} + c\beta_{N,4N\pi}, 0),$$

with

$$P_r(x) = \frac{1}{\pi} \frac{r}{x^2 + r^2}$$

the Poisson kernel for the half-plane (note that $P_r * \text{Id}_{\mathbb{R}} = \text{Id}_{\mathbb{R}}$) and $\beta_{N,y}(x) = \beta_N(x - y)$, where β_N is the (unique and $8N\pi$ -periodic) primitive of

$$\frac{1}{8N\pi} - \sum_{n \in \mathbb{Z}} \delta_{8N\pi n}$$

which has $\int_{-4N\pi}^{4N\pi} \beta_N(x) dx = 0$. This and the smoothness of ϕ means $z_{N,A,r,a,c}(\cdot, 0)$ can be extended analytically to the strip $S_r = \mathbb{R} \times [-r, r]$ and this extension satisfies for each $k \geq 0$,

$$\sup_{\substack{N \geq 1, A \in [1.08050, 1.08055] \\ r, a, c \in [0, 1/2], |\zeta| \leq r}} \|\partial_x^k z_{N,A,r,a,c}(\cdot + i\zeta, 0)\|_{L^\infty} < \infty.$$

Before we continue, let us discuss the different components of the function $z_{N,A,r,a,c}(\cdot, 0)$. First, $\bar{z}_{N,A}$ is just a smooth version of the function from (2-4), and we convolve it with P_r because we need the initial condition to be analytic. Since $\partial_x \bar{z}_{N,A}^1 \geq 0$, this yields $\partial_x z_{N,A,r,a,c}(\cdot, 0) > 0$ for any $r > 0$. That would mean that for a short (positive and negative) time, the solution would remain stable everywhere—in particular, near $x = 2n\pi$ for any integer n with $|n| \in (0, 2N) \setminus \{N\}$ as we want (see above). However, we do not want this to be the case near $x \in 2N\pi\mathbb{Z}$, which is where the term $P_1 * (\cdot \cdot \cdot)$ comes in. It is analytic and we will choose a, c to be close to the unique $a_{N,r} > 0$ such that (2-9) and (2-10) below hold. In fact, we will have $a = a_{N,r} - \delta$ and $c = a_{N,r} - \varepsilon$ for some small $0 < \delta \approx 3\varepsilon / (8N - 1) \ll 1$, chosen so that $\partial_x z_{N,A,r,a,c}^1(x, 0) > 0$ for $x \in 2N\pi\mathbb{Z} \setminus 8N\pi\mathbb{Z}$ and (2-12) holds. We will then finally choose $A = A_{N,r,\delta,\varepsilon} \in (1.08050, 1.08055)$ so that (2-11) also holds, and all this will ensure that $z_{N,A,r,a,c}$

undergoes the stability shifts described after (2-4). We note that we will first have to choose N large and $r > 0$ small so that (2-5), (2-6), and (2-8) below hold for all $a, c \approx a_{N,r}$ (which is small if r is). This will then specify $a_{N,r}$, after which sufficiently small ε, δ will be chosen and they will determine $A_{N,r,\delta,\varepsilon}$.

The proof of Theorem 5.1 in [Castro et al. 2012] shows that for each $r > 0$ there is T_r (depending only on r) such that (1-4) has a unique analytic solution $z_{N,A,r,a,c}$ on the time interval $(-T_r, T_r)$ with initial condition $z_{N,A,r,a,c}(\cdot, 0)$ (moreover, $\partial_t z_{N,A,r,a,c}$ is also analytic), and this satisfies for each $k \geq 0$,

$$\sup_{\substack{N \geq 1, A \in [1.08050, 1.08055] \\ r, a, c \in [0, 1/2], |t| < T_r}} (\|\partial_x^k z_{N,A,r,a,c}(\cdot, t)\|_{L^\infty} + \|\partial_t \partial_x^k z_{N,A,r,a,c}(\cdot, t)\|_{L^\infty}) < \infty.$$

Below we always consider $A \in [1.08050, 1.08055]$ and $r, a, c \in [0, \frac{1}{2}]$.

This means that the bound (2-2) extends to each $z_{N,A,r,a,c}$ and $(x, t) \in \mathbb{R} \times (-T_r, T_r)$ (where $T_0 = 0$), with a uniform C . We also have

$$\partial_t \partial_x z_{N,A,r,a,c}^1(4N\pi, 0) \geq 10^{-6} \quad \text{and} \quad \partial_t \partial_x z_{N,A,r,a,c}^1(\pm 2N\pi, 0) \leq -10^{-6}, \tag{2-5}$$

as well as

$$\partial_t \partial_x z_{N,1.08050,r,a,c}^1(0, 0) \geq 10^{-6} \quad \text{and} \quad \partial_t \partial_x z_{N,1.08055,r,a,c}^1(0, 0) \leq -10^{-6}, \tag{2-6}$$

both when $N^{-1} + r + a + c$ is small enough. This follows from the bounds (2-3) and from

$$\|\partial_x^k z_{N,A,r,a,c}(\cdot, 0) - \partial_x^k \bar{z}_{N,A}\|_{L^\infty(I_N)} \rightarrow 0 \quad \text{as} \quad N^{-1} + r + a + c \rightarrow 0 \tag{2-7}$$

for each k , where $I_N = \bigcup_{n \in \mathbb{Z}} (2N\pi n - N, 2N\pi n + N)$. Similarly, (2-2) and (2-7) also prove

$$\partial_{tt} \partial_x z_{N,A,r,a,c}^1(0, 0) \geq 20 \tag{2-8}$$

for small enough $N^{-1} + r + a + c$. Fix now N so that (2-5), (2-6), and (2-8) hold for all small enough $r + a + c$.

We next notice that for each $r > 0$ we have $\partial_x z_{N,A,r,0,0}^1(x) = 1 - (P_r * \cos)(x)$, which is a 2π -periodic function with a positive minimum at $x = 0$ (independent of N, A). Thus there is a unique $a_{N,r} > 0$ (small if $r > 0$ is small) such that

$$\partial_x z_{N,A,r,a_{N,r},a_{N,r}}^1(2N\pi n, 0) = 0 \tag{2-9}$$

for each $n \in \mathbb{Z}$, and

$$\partial_x z_{N,A,r,a_{N,r},a_{N,r}}^1(x, 0) > 0 \tag{2-10}$$

for $x \notin 2N\pi\mathbb{Z}$. Finally, for any $\delta, \varepsilon \in [0, a_{N,r})$ let $A_{N,r,\delta,\varepsilon} \in (1.08050, 1.08055)$ be such that

$$\partial_t \partial_x z_{N,A_{N,r,\delta,\varepsilon},r,a_{N,r}-\delta,a_{N,r}-\varepsilon}^1(0, 0) = 0, \tag{2-11}$$

which exists due to (2-6) and the continuity of $\partial_t \partial_x z_{N,A_{N,r,\delta,\varepsilon},r,a_{N,r}-\delta,a_{N,r}-\varepsilon}^1(0, 0)$ in A .

For the sake of simplicity of notation, define $z = z_{N,A_{N,r,\delta,\varepsilon},r,a_{N,r}-\delta,a_{N,r}-\varepsilon}$. We now let $r > 0$ be small enough, and then pick $\delta, \varepsilon \in (0, a_{N,r})$ small enough (we will need $\varepsilon \ll 10^{-6}T_r$, see below) such that

$$0 < -\partial_x z^1(0, 0) \ll \left[\frac{1}{C} \min_{n \in \{-1, 1, 2\}} \partial_x z^1(2N\pi n, 0) \right]^2, \tag{2-12}$$

with C the constant from (2-2) for $z_{N,A,r,a,c}$. (That is, $\varepsilon > 0$ is chosen small and δ slightly smaller than the value that makes $\partial_x z^1(0, 0) = 0$ for this ε , which means that

$$\delta = \frac{3\varepsilon}{8N-1} - O\left(\frac{\varepsilon}{N^2}\right);$$

moreover, then all three values inside the min are $\approx \varepsilon/\pi$.) Then we claim that this z is the desired solution. Indeed, $\partial_x z^1(0, t) < 0$ for all small enough $|t|$ and the argument from the proof of Theorem 2.1 shows that $\partial_x z^1(x, t) > 0$ for all $x \in \mathbb{R}$ when

$$|\partial_x z^1(0, 0)|^{1/2} \ll |t| \ll \frac{\varepsilon}{C\pi}.$$

Finally, (2-5) and a uniform bound on $\partial_t^2 \partial_x z^1_{N,A,r,a,c}$ (obtained similarly to (2-2)) show that

$$\partial_x z^1(4N\pi, -t) < 0 \quad \text{and} \quad \partial_x z^1(\pm 2N\pi, t) < 0$$

for all $t \approx 10^6\varepsilon$ if $\varepsilon \ll 10^{-6}T_r$ is small enough (because $\partial_x z^1(4N\pi, 0) \approx \varepsilon/\pi \approx \partial_x z^1(\pm 2N\pi, 0)$).

We thus proved the following result.

Theorem 2.3. *There exist $T > T' > \gamma > 0$ and a spatially analytic solution z to (1-5) on the time interval $[-T, T]$ such that $z(\cdot, t)$ is a graph of a smooth function of x when $|t| \in [T' - \gamma, T' + \gamma]$ but $z(\cdot, t)$ is not a graph of a function of x when $|t| \in [0, \gamma] \cup [T - \gamma, T]$.*

3. Technical details of the numerical implementation

In this section, we give some technical details of the implementation of the computer-assisted part of the proof of Lemma 2.2. In order to perform the rigorous computations we used the C-XSC library [Hofschuster and Krämer 2004]. We refer the reader to the appendices, found in the online supplement, to see a detailed expression of the integral terms involved in the calculations. For the sake of readability, we kept the same names for the integrals in the paper and in the code. The code can also be found in the online supplement.

The implementation is split into several files, and many of the headers of the functions (such as the integration methods) contain pointers to functions (the integrands) so that they can be reused for an arbitrary number of integrals with minimal changes and easy and safe debugging. For the sake of clarity, and at the cost of numerical performance and duplicity in the code, we decided to treat many simple integrals instead of a single big one.

We start discussing the details of the first part of Lemma 2.2, corresponding to the one-dimensional integrals. The three integrals can be found in Appendix A. We split them into two parts: a nonsingular one over the interval $[\delta, \pi]$ and a singular one over the interval $[0, \delta]$. The nonsingular part is calculated using a Gauss–Legendre quadrature of order 2, given by

$$\int_a^b f(\eta) d\eta \in \frac{b-a}{2} \left(f\left(\frac{b-a}{2} \frac{\sqrt{3}}{3} + \frac{b+a}{2}\right) + f\left(-\frac{b-a}{2} \frac{\sqrt{3}}{3} + \frac{b+a}{2}\right) \right) + \frac{1}{4320} (b-a)^5 f^4([a, b]).$$

Moreover, the integration is done in an adaptive way. For each region, we accepted or rejected the result depending on the width in an absolute and a relative way. It is important to notice that because of the

uncertainty in ε and/or overestimation, division by zero might occur, even in small integration intervals. We used $\delta = 2^{-9}$ and tolerances `AbsTol` and `RelTol` equal to 10^{-6} .

In the singular region, the singularity around $y = 0$ is integrable; hence the integral is finite. We performed a Taylor expansion around $y = 0$ in both the numerator and denominator (resp. of orders 2, 2 and 4 for A_1 , A_2 and A_3), simplified the powers of y and then integrated. Potentially this could fail because the uncertainty in the parameters or overestimation could yield a Taylor series in which 0 belongs to the coefficient of the first nonsimplified power of the denominator. Whenever this happens, we try to integrate instead using a Gauss–Legendre quadrature of order 2.

The maximum number of subdivision levels was 18 (2^{18} intervals) for the bounded region and 12 (2^{12} intervals) for the singular one. The splitting of the intervals is done in an arithmetic way; i.e, we split an integration interval $[a, b]$ into $[a, \frac{1}{2}(a + b)]$ and $[\frac{1}{2}(a + b), b]$.

In the second part of Lemma 2.2 we have to deal with 41 two-dimensional integrals (see Appendix B for a detailed list of them and their derivation). The first step is to exploit the symmetry of the integrands in (y, z) -variables to integrate only over the region $[0, \pi] \times [-\pi, \pi]$. We will distinguish four different regions labeled in the following way: nonsingular $([\delta, \pi] \times [\delta, \pi]) \cup ([\delta, \pi] \times [-\pi, -\delta])$, singular-first-coordinate $([0, \delta] \times [\delta, \pi]) \cup ([0, \delta] \times [-\pi, -\delta])$, singular-second-coordinate $[\delta, \pi] \times [-\delta, \delta]$ and singular-center $[0, \delta] \times [-\delta, \delta]$.

The nonsingular region was integrated as before, using a 2D Gauss–Legendre quadrature of order 2. The singular-center region was integrated in the following way. Assuming $\text{sign}(a) = \text{sign}(b)$, $\text{sign}(c) = \text{sign}(d)$ and that we expand up to orders `num_y`, `den_y`, `num_z`, `den_z`:

$$\begin{aligned} \int_a^b \int_c^d \frac{\text{Num}(y, z)}{\text{Den}(y, z)} dy dz &\in \int_a^b \int_c^d \frac{\frac{1}{\text{num_y!num_z!}} \partial_y^{\text{num_y}} \partial_z^{\text{num_z}} \text{Num}(A, B) y^{\text{num_y}} z^{\text{num_z}}}{\frac{1}{\text{den_y!den_z!}} \partial_y^{\text{den_y}} \partial_z^{\text{den_z}} \text{Den}(A, B) y^{\text{den_y}} z^{\text{den_z}}} dy dz \\ &= \frac{1}{1 + \text{num_y} - \text{den_y}} \frac{1}{1 + \text{num_z} - \text{den_z}} \frac{\text{den_y!den_z!}}{\text{num_y!num_z!}} \\ &\quad \times \frac{\partial_y^{\text{num_y}} \partial_z^{\text{num_z}} \text{Num}(A, B)}{\partial_y^{\text{den_y}} \partial_z^{\text{den_z}} \text{Den}(A, B)} y^{1+\text{num_y}-\text{den_y}} z^{1+\text{num_z}-\text{den_z}} \Bigg|_{z=c}^{z=d} \Bigg|_{y=a}^{y=b}, \end{aligned}$$

where A is the convex hull of $\{0, a, b\}$ and B is the convex hull of $\{0, c, d\}$. For the singular-first-coordinate and singular-second-coordinate regions the same procedure was applied taking `num_z` = `den_z` = 0, $B = [c, d]$ and `num_y` = `den_y` = 0, $A = [a, b]$ respectively. A detailed list of the orders of each of the integrals can be found in Table 1 in Appendix C. Whenever the Taylor-based formulas failed because of 0 being enclosed in the denominator terms, we tried to integrate using 2D Gauss–Legendre of order 2.

In this two-dimensional setting, we used a geometric splitting (in both coordinates) in the nonsingular region, arithmetic in the singular-center and singular-first-coordinate and hybrid in the singular-second-coordinate (see below). The geometric splitting consists in splitting by the geometric mean as opposed to the arithmetic one (i.e., assuming a and b have the same sign and are nonzero, we split $[a, b]$ into $[a, \sqrt{ab} \text{sign}(a)]$ and $[\sqrt{ab} \text{sign}(a), b]$). While the arithmetic division minimizes the length of the longest piece after the division, the geometric one minimizes the piece with the biggest ratio between its endpoints.

This can be particularly useful in many cases: for example in order to avoid divisions by zero for integrands of the type $1/(y - A \sin(y))$, which is a simplified version of some of the denominators that appear in all the terms. Detailed results of the breakdown by region and by term can be found in Table 2 of Appendix C.

We chose $\delta = 2^{-5}$, and `AbsTo1` and `Re1To1` equal to 10^{-4} . We changed the number of maximum subdivision levels depending on the region and (possibly) depending on the terms. For the nonsingular region, the maximum number was 10 (2^{20} intervals). In the singular-first-coordinate, the maximum number of subdivisions was 8 (2^{16} intervals), and that number was also used in the singular-center region. The singular-second-coordinate region was treated differently: all terms other than B_{47} and B_{55} were further split into three subregions: $[\delta, 0.65] \times [-\delta, \delta]$, $[0.65, 0.95] \times [-\delta, \delta]$ and $[0.95, \pi] \times [-\delta, \delta]$ and setting the maximum number of subdivisions to 9 in each subregion. The first and second subregions were computed using arithmetic splitting, whereas the third one was split geometrically only in the first coordinate, and arithmetically in the second.

The singular-second-coordinate regions of the terms B_{47} and B_{55} are highly singular because of the cubic denominators and they required special precision. They were subdivided into six subregions: namely $[\delta, 0.325] \times [-\delta, \delta]$, $[0.325, 0.65] \times [-\delta, \delta]$, $[0.65, 0.775] \times [-\delta, \delta]$, $[0.775, 0.95] \times [-\delta, \delta]$, $[0.95, 1.5] \times [-\delta, \delta]$ and $[1.5, \pi] \times [-\delta, \delta]$. The maximum number of subdivisions was 10 in each subregion. The last two subregions were split geometrically in the first coordinate, arithmetically in the second. The other four subregions were split arithmetically in each of the coordinates.

The simulations were run on the NewComp cluster at Princeton University. Each of the programs was run on a core of 2 Xeon X5680 CPUs (6 cores each, 12 in total) at 3.33 GHz and 8 GB of RAM. The total runtime was about 3.5 min for the first part of Lemma 2.2. For the second part, the different runtimes are summarized in Table 3 of Appendix C.

Acknowledgements

Córdoba and Gómez-Serrano were partially supported by the grant MTM2014-59488-P (Spain) and ICMAT Severo Ochoa project SEV-2011-0087. Gómez-Serrano was partially supported by an AMS-Simons Travel Grant. Zlatoš acknowledges partial support by NSF grants DMS-1652284 and DMS-1656269. We thank Princeton University for computing facilities (NewComp cluster). We are also very grateful to the anonymous referees for their valuable comments and suggestions.

References

- [Berselli et al. 2014] L. C. Berselli, D. Córdoba, and R. Granero-Belinchón, “Local solvability and turning for the inhomogeneous Muskat problem”, *Interfaces Free Bound.* **16**:2 (2014), 175–213. MR Zbl
- [Berz and Makino 1999] M. Berz and K. Makino, “New methods for high-dimensional verified quadrature”, *Reliab. Comput.* **5**:1 (1999), 13–22. MR Zbl
- [Castro et al. 2012] Á. Castro, D. Córdoba, C. Fefferman, F. Gancedo, and M. López-Fernández, “Rayleigh–Taylor breakdown for the Muskat problem with applications to water waves”, *Ann. of Math. (2)* **175**:2 (2012), 909–948. MR Zbl
- [Castro et al. 2013] Á. Castro, D. Córdoba, C. Fefferman, and F. Gancedo, “Breakdown of smoothness for the Muskat problem”, *Arch. Ration. Mech. Anal.* **208**:3 (2013), 805–909. MR Zbl

- [Cheng et al. 2016] C. H. A. Cheng, R. Granero-Belinchón, and S. Shkoller, “Well-posedness of the Muskat problem with H^2 initial data”, *Adv. Math.* **286** (2016), 32–104. MR Zbl
- [Constantin et al. 2013] P. Constantin, D. Córdoba, F. Gancedo, and R. M. Strain, “On the global existence for the Muskat problem”, *J. Eur. Math. Soc. (JEMS)* **15**:1 (2013), 201–227. MR Zbl
- [Constantin et al. 2016a] P. Constantin, D. Córdoba, F. Gancedo, L. Rodríguez-Piazza, and R. M. Strain, “On the Muskat problem: global in time results in 2D and 3D”, *Amer. J. Math.* **138**:6 (2016), 1455–1494.
- [Constantin et al. 2016b] P. Constantin, F. Gancedo, R. Shvydkoy, and V. Vicol, “Global regularity for 2D Muskat equations with finite slope”, *Ann. Inst. H. Poincaré Anal. Non Linéaire* (online publication September 2016).
- [Córdoba and Gancedo 2007] D. Córdoba and F. Gancedo, “Contour dynamics of incompressible 3-D fluids in a porous medium with different densities”, *Commun. Math. Phys.* **273**:2 (2007), 445–471. MR Zbl
- [Córdoba and Gancedo 2009] D. Córdoba and F. Gancedo, “A maximum principle for the Muskat problem for fluids with different densities”, *Comm. Math. Phys.* **286**:2 (2009), 681–696. MR Zbl
- [Córdoba et al. 2015] D. Córdoba, J. Gómez-Serrano, and A. Zlatoš, “A note on stability shifting for the Muskat problem”, *Philos. Trans. Roy. Soc. A* **373**:2050 (2015), art. id. 20140278. MR Zbl
- [Escher and Matioc 2011] J. Escher and B.-V. Matioc, “On the parabolicity of the Muskat problem: well-posedness, fingering, and stability results”, *Z. Anal. Anwend.* **30**:2 (2011), 193–218. MR Zbl
- [Friedman and Tao 2003] A. Friedman and Y. Tao, “Nonlinear stability of the Muskat problem with capillary pressure at the free boundary”, *Nonlinear Anal.* **53**:1 (2003), 45–80. MR Zbl
- [Gómez-Serrano and Granero-Belinchón 2014] J. Gómez-Serrano and R. Granero-Belinchón, “On turning waves for the inhomogeneous Muskat problem: a computer-assisted proof”, *Nonlinearity* **27**:6 (2014), 1471–1498. MR Zbl
- [Granero-Belinchón 2014] R. Granero-Belinchón, “Global existence for the confined Muskat problem”, *SIAM J. Math. Anal.* **46**:2 (2014), 1651–1680. MR Zbl
- [Hofschuster and Krämer 2004] W. Hofschuster and W. Krämer, “C-XSC 2.0 — a C++ library for extended scientific computing”, pp. 15–35 in *Numerical software with result verification* (Dagstuhl, Germany, 2003), edited by R. Alt et al., Springer, Berlin, 2004.
- [Krämer and Wedner 1996] W. Krämer and S. Wedner, “Two adaptive Gauss–Legendre type algorithms for the verified computation of definite integrals”, *Reliab. Comput./Nadezhn. Vychisl.* **2**:3 (1996), 241–253. MR Zbl
- [Lang 2001] B. Lang, “Derivative-based subdivision in multi-dimensional verified gaussian quadrature”, pp. 145–152 in *Symbolic algebraic methods and verification methods* (Dagstuhl, Germany, 1999), edited by G. Alefeld et al., Springer, Vienna, 2001. MR Zbl
- [Moore 1979] R. Moore, *Methods and applications of interval analysis*, Studies in applied and numerical mathematics **2**, SIAM, Philadelphia, PA, 1979. MR Zbl
- [Muskat 1937] M. Muskat, “The flow of fluids through porous media”, *J. Appl. Phys.* **8**:4 (1937), 274–282. Zbl
- [Siegel et al. 2004] M. Siegel, R. E. Caffisch, and S. Howison, “Global existence, singular solutions, and ill-posedness for the Muskat problem”, *Comm. Pure Appl. Math.* **57**:10 (2004), 1374–1411. MR Zbl
- [Tucker 2011] W. Tucker, *Validated numerics: a short introduction to rigorous computations*, Princeton University Press, 2011. MR Zbl

Received 27 Jan 2016. Revised 26 Oct 2016. Accepted 26 Dec 2016.

DIEGO CÓRDOBA: dcg@icmat.es

Instituto de Ciencias Matemáticas, Consejo Superior de Investigaciones Científicas, c/ Nicolas Cabrera, 13-15 Campus Cantoblanco UAM, 28049 Madrid, Spain

JAVIER GÓMEZ-SERRANO: jg27@math.princeton.edu

Department of Mathematics, Princeton University, 610 Fine Hall, Washington Rd, Princeton, NJ 08544, United States

ANDREJ ZLATOŠ: zlatos@ucsd.edu

Department of Mathematics, University California San Diego, 9500 Gilman Dr. #0112, La Jolla, CA 92093, United States

Analysis & PDE

msp.org/apde

EDITORS

EDITOR-IN-CHIEF

Patrick Gérard
patrick.gerard@math.u-psud.fr
Université Paris Sud XI
Orsay, France

BOARD OF EDITORS

| | | | |
|----------------------|---|-----------------------|--|
| Nicolas Burq | Université Paris-Sud 11, France nicolas.burq@math.u-psud.fr | Werner Müller | Universität Bonn, Germany mueller@math.uni-bonn.de |
| Massimiliano Berti | Scuola Intern. Sup. di Studi Avanzati, Italy berti@sissa.it | Gilles Pisier | Texas A&M University, and Paris 6 pisier@math.tamu.edu |
| Sun-Yung Alice Chang | Princeton University, USA chang@math.princeton.edu | Tristan Rivière | ETH, Switzerland riviere@math.ethz.ch |
| Michael Christ | University of California, Berkeley, USA mchrist@math.berkeley.edu | Igor Rodnianski | Princeton University, USA irod@math.princeton.edu |
| Charles Fefferman | Princeton University, USA cf@math.princeton.edu | Wilhelm Schlag | University of Chicago, USA schlag@math.uchicago.edu |
| Ursula Hamenstaedt | Universität Bonn, Germany ursula@math.uni-bonn.de | Sylvia Serfaty | New York University, USA serfaty@cims.nyu.edu |
| Vaughan Jones | U.C. Berkeley & Vanderbilt University vaughan.f.jones@vanderbilt.edu | Yum-Tong Siu | Harvard University, USA siu@math.harvard.edu |
| Vadim Kaloshin | University of Maryland, USA vadim.kaloshin@gmail.com | Terence Tao | University of California, Los Angeles, USA tao@math.ucla.edu |
| Herbert Koch | Universität Bonn, Germany koch@math.uni-bonn.de | Michael E. Taylor | Univ. of North Carolina, Chapel Hill, USA met@math.unc.edu |
| Izabella Laba | University of British Columbia, Canada ilaba@math.ubc.ca | Gunther Uhlmann | University of Washington, USA gunther@math.washington.edu |
| Gilles Lebeau | Université de Nice Sophia Antipolis, France lebeau@unice.fr | András Vasy | Stanford University, USA andras@math.stanford.edu |
| Richard B. Melrose | Massachusetts Inst. of Tech., USA rbm@math.mit.edu | Dan Virgil Voiculescu | University of California, Berkeley, USA dvv@math.berkeley.edu |
| Frank Merle | Université de Cergy-Pontoise, France Frank.Merle@u-cergy.fr | Steven Zelditch | Northwestern University, USA zelditch@math.northwestern.edu |
| William Minicozzi II | Johns Hopkins University, USA minicozz@math.jhu.edu | Maciej Zworski | University of California, Berkeley, USA zworski@math.berkeley.edu |
| Clément Mouhot | Cambridge University, UK c.mouhot@dpms.cam.ac.uk | | |

PRODUCTION

production@msp.org
Silvio Levy, Scientific Editor

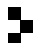
See inside back cover or msp.org/apde for submission instructions.

The subscription price for 2017 is US \$265/year for the electronic version, and \$470/year (+\$55, if shipping outside the US) for print and electronic. Subscriptions, requests for back issues from the last three years and changes of subscribers address should be sent to MSP.

Analysis & PDE (ISSN 1948-206X electronic, 2157-5045 printed) at Mathematical Sciences Publishers, 798 Evans Hall #3840, c/o University of California, Berkeley, CA 94720-3840, is published continuously online. Periodical rate postage paid at Berkeley, CA 94704, and additional mailing offices.

APDE peer review and production are managed by EditFlow® from MSP.

PUBLISHED BY

 **mathematical sciences publishers**
nonprofit scientific publishing

<http://msp.org/>

© 2017 Mathematical Sciences Publishers

ANALYSIS & PDE

Volume 10 No. 2 2017

| | |
|--|-----|
| Some energy inequalities involving fractional GJMS operators JEFFREY S. CASE | 253 |
| Exact controllability for quasilinear perturbations of KdV PIETRO BALDI, GIUSEPPE FLORIDIA and EMANUELE HAUS | 281 |
| Operators of subprincipal type NILS DENCKER | 323 |
| Anisotropic Ornstein nonequalities KRYSTIAN KAZANIECKI, DMITRIY M. STOLYAROV and MICHAŁ WOJCIECHOWSKI | 351 |
| A note on stability shifting for the Muskat problem, II: From stable to unstable and back to stable DIEGO CÓRDOBA, JAVIER GÓMEZ-SERRANO and ANDREJ ZLATOŠ | 367 |
| Derivation of an effective evolution equation for a strongly coupled polaron RUPERT L. FRANK and ZHOU GANG | 379 |
| Time-weighted estimates in Lorentz spaces and self-similarity for wave equations with singular potentials MARCELO F. DE ALMEIDA and LUCAS C. F. FERREIRA | 423 |
| Optimal well-posedness for the inhomogeneous incompressible Navier–Stokes system with general viscosity COSMIN BURTEA | 439 |
| Global dynamics below the standing waves for the focusing semilinear Schrödinger equation with a repulsive Dirac delta potential MASAHIRO IKEDA and TAKAHISA INUI | 481 |



2157-5045(2017)10:2;1-W